ChemComm
Chemical Communications

Accepted Manuscript

This article can be cited before page numbers have been issued, to do this please use: Y. He, J. Yu, X. Hu, S. Huang, L. Cai, L. Yang, H. Zhang, Y. Jiang, Y. Jia and H. Sun, *Chem. Commun.*, 2020, DOI: 10.1039/D0CC06129H.

ROYAL SOCIETY OF CHEMISTRY

rsc.li/chemcomm

View Article Online
DOI: 10.1039/D0CC06129H

COMMUNICATION

An activity-based fluorescent probe and its application for differentiating alkaline phosphatase activity in different cell lines

Received 00th January 20xx,
Accepted 00th January 20xx

DOI: 10.1039/x0xx00000x

Yong He,[a‡] Junli Yu,[b‡] Xiangzi Hu,[a‡] Shumei Huang,[a] Lili Cai,[a] Liu Yang,[c,d] Huatang Zhang,[a*] Yin Jiang,[a*] Yongguang Jia,[e] Hongyan Sun[c,d*]

Herein, a new fluorescent probe, AE-Phos, is reported for detecting ALP activity with the combined advantages of aggregation-induced emission (AIE) and excited state intramolecular proton transfer (ESIPT). Further detailed fluorescence experiments demonstrated that AE-Phos exhibited excellent selectivity and sensitivity, large Stokes shift, and fast response towards ALP. Furthermore, AE-Phos was applied to imaging ALP activity in different cell lines quantitatively.

Alkaline phosphatases (ALPs) are a family of enzymes, which regulate the phosphate metabolism and exist widely in both of the prokaryotes and eukaryotes.[1] Through the catalyse reaction of dephosphorylation under alkaline pH environment, ALP is responsible for regulating a lot of momentous biological processes.[2] In some serious diseases such as cirrhosis, hepatitis, hyperparathyroidism, Hodgkin's lymphoma and liver cancer, the elevated ALP activity levels in serum is a very common phenomenon.[3] Therefore, it is highly desirable to develop the chemical tools that can detect ALP activity in living systems accurately and selectively.

The fluorescent probes have captured the attention due to their high sensitivity and noninvasiveness, which allow them to be effective for *in vitro* and *in vivo* studies with minimal perturbation.[4] Several research groups including us have reported a number of fluorescent probes for detecting and visualizing ALP activity in biological system.[5] However, these probes are based on the conventional fluorescent scaffolds and suffer from aggregation-caused quenching (ACQ) when amassed in cells. In addition, the traditional "turn-on" probes show obvious intrinsic fluorescence, which affects the detection sensitivity. Most traditional fluorophores for designing ALP probes also suffer from potential self-reabsorption, photo-bleaching and background fluorescence interference because of the short Stokes shift.

Fluorophores with AIE property have received increasing attention in the field of biosensing and imaging during the past two decades.[6] AIE fluorophores are non-emissive when dissolved in solution freely but become highly emissive in the state of aggregation. ESIPT is a photochemical process that occurs in the excited singlet state of a fluorophore with intramolecular hydrogen bond.[7] Because of its unique and transient four-level photochemical process, ESIPT fluorophores usually display a number of advantages compared with traditional fluorophores (fluorescein, rhodamine, etc.), such as large Stokes shift and local environment sensitiveness.[7a] Therefore, it will be highly desirable to design fluorophores with both AIE and ESIPT characteristics.

In this study, we intend to design new fluorescent probes for ALP imaging that possess both characteristics of AIE and ESIPT. In 2009, Tong et al. reported a sequence of salicylaldehyde azine (SA) derivatives that exhibited AIE enhancement and ESIPT characteristics.[8] Recently, Tong and Liu et al. have designed several fluorescent probes based on the scaffold of SA with AIE+ESIPT mechanism.[9] Inspired by these pioneering works, we develop a new fluorescent probe, **AE-Phos**, for ALP detection and imaging in living cells. As shown in Scheme 1, the hydroxyl groups in **AE-Phos**, which is the crucial element for AIE and ESIPT properties, is protected with the phosphate group. The introduction of phosphate group endowed the probe with excellent water solubility and prevent the formation of ESIPT and AIE, leading to dramatic quenching of background fluorescence. In the existence of ALP, the phosphate group is

[a.] *School of Chemical Engineering and Light Industry and School of Biomedical and Pharmaceutical Sciences, Guangdong University of Technology, Guangzhou, Guangdong, 510006, China. E-mail: htzhang@gdut.edu.cn; junhe@gdut.edu.cn*
[b.] *Department of Ultrasonography, The Sixth Affiliated Hospital of Sun Yat-sen University, Guangzhou, 510655, China*
[c.] *Department of Chemistry and Center of Super-Diamond and Advanced Films (COSDAF), City University of Hong Kong, 83 Tat Chee Avenue, Kowloon, Hong Kong, China. E-mail: hongysun@cityu.edu.hk*
[d.] *Chengdu Research Institute, City University of Hong Kong, Chengdu, 610200, China.*
[e.] *National Engineering Research Center for Tissue Restoration and Reconstruction, South China University of Technology, Guangzhou 510006, China.*
‡These authors contributed equally.
Electronic Supplementary Information (ESI) available: [details of any supplementary information available should be included here]. See DOI: 10.1039/x0xx00000x

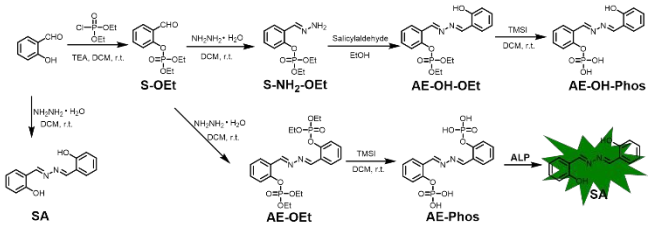

Scheme 1 Synthesis route of SA, AE-OH-Phos, **AE-Phos** and the reaction mechanism with ALP.

and the hydroxyl groups are recovered, resulting in the formation of the fluorescent compound SA with AIE+ESIPT characteristics. Compared with traditional ALP probes, **AE-Phos** shows extremely low background fluorescence and high fluorescent enhancement ratio due to the combined judicious characteristics of AIE+ESIPT and the large Stokes shift. In addition, we have successfully used the probe to differentiate endogenous ALP activity in different cell lines by confocal microscopy.

AE-Phos was synthesized according to the procedure illustrated in Scheme 1 and S1. The uncaged product (SA) and the intermediate product (AE-OH-Phos) were also synthesized to examine the dephosphorylation mechanism of ALP. The probe and the control compounds have been synthesized and characterized by ^{1}H NMR, ^{13}C NMR and ^{31}P NMR in detail (Supporting Information, ESI†).

The UV absorption and the fluorescent emission of SA, which is the theoretical reaction product of **AE-Phos** and ALP, were first measured in DMSO and water. SA dissolved well in DMSO but it was not soluble in water. The maximum absorption wavelength of SA was 356 nm. The fluorescence intensity of SA enhanced when the water fraction increased. AIE effect was observed when the water fraction was over 60% (Fig. 1A and S1A). On the other hand, **AE-Phos** did not display fluorescence emission from 0%-100% water fractions even though it dissolved well both in water and DMSO (Fig. 1A and S1B). It is noteworthy that a remarkable Stokes shift (180 nm) was observed for SA. This is attributed to ESIPT mechanism (Fig. 1B). The combined AIE and ESIPT effect not only reduce self-quenching of fluorophore, but also improve the sensitivity of fluorescence measurement drastically. In addition, we also tested the fluorescence stability of **AE-Phos** and SA. As shown in Fig. S2, the fluorescence intensities of **AE-Phos** and SA remained unchanged over 120 min, indicating that both compounds possess excellent stability in 100% water.

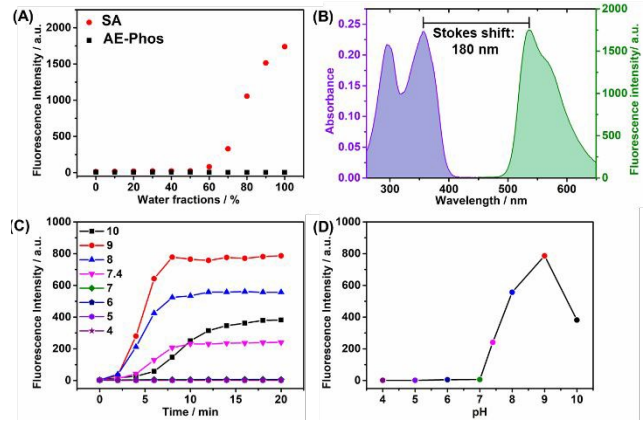

Fig. 1 (A) Fluorescence intensity of SA (5 μM) and **AE-Phos** (5 μM) at 536 nm with different water fractions; (B) UV-vis absorption and fluorescence emission spectra of SA in Tris buffer; (C) Time-dependent fluorescence response of **AE-Phos** toward ALP (100 U/L) in Tris buffer (50 mM) at different pHs at 37 ºC; (D) Plot of fluorescence intensity with 536 nm **AE-Phos** (5 μM) after incubation with ALP (100 U/L) at 37 ºC for 30 min at different pH values. Ex:356 nm.

It is well known that the enzymatic activity of ALP is pH sensitive. We therefore measured the effect of pH on the reaction kinetic of **AE-Phos** with ALP. As shown in Fig. 1C and S3, the fluorescence intensity of the reaction solution displayed no obvious changes in the pH range of 4 to 7 when **AE-Phos** was incubated with ALP for 20 min. This result was due to the low enzymatic activity of ALP under acidic condition.[10] However, when the pH values were higher than 7, the fluorescent intensity increased significantly with increasing pH value. It was noted that the fluorescent intensity at pH 10 was lower than those at pH 8 and 9. The phenomenon is not due to the lower reaction kinetic of ALP at pH 10. It is attributed to the deprotonation of the reaction product SA, which forms negatively charged ions and is released from aggregates to form weakly fluorescent monomers.[8] Therefore, we chose pure Tris buffer of pH 9.0 as the testing condition in the following experiment (Fig. 1D).

Then, the reaction kinetics of **AE-Phos** with ALP was investigated. The fluorescence spectra variation over time was recorded in the presence of **AE-Phos** (5 μM) and a range of different concentration of ALP (0-100 U/L) in Tris buffer. As expected, the fluorescence intensity was enhanced in response to increasing ALP concentration (Fig. 2A and S4). The fluorescence intensity generally plateaued within 10 min. The faster reaction kinetics has been observed at higher ALP concentrations indicates higher cleavage reaction rate. We also monitored the variation of fluorescence intensity with fixed concentration of ALP (100 U/L) and different concentrations of **AE-Phos** (0.1 to 20 μM). The fluorescent measurement data with a given probe concentration at first 120 seconds is displayed in Fig. 2B. These fluorescence intensities are utilized to calculate the initial reaction rate (V_0) at different concentrations of probe (Fig. S5). Km and Vmax are calculated respectively to be 7.66 μM and 0.408 μM/min based on the Linewaver-Burk analysis. These values are comparable to those previously reported fluorescent probes (Table S1).

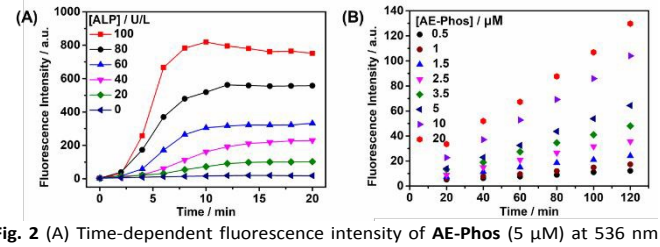

Fig. 2 (A) Time-dependent fluorescence intensity of **AE-Phos** (5 μM) at 536 nm with various concentrations of ALP (0-100 U/L); (B) Plots of the fluorescence intensity at 536 nm versus incubation time under different concentrations of **AE-Phos** (0.5-20 μM) with 100 U/L ALP in Tris buffer (pH 9.0, 50 mM).

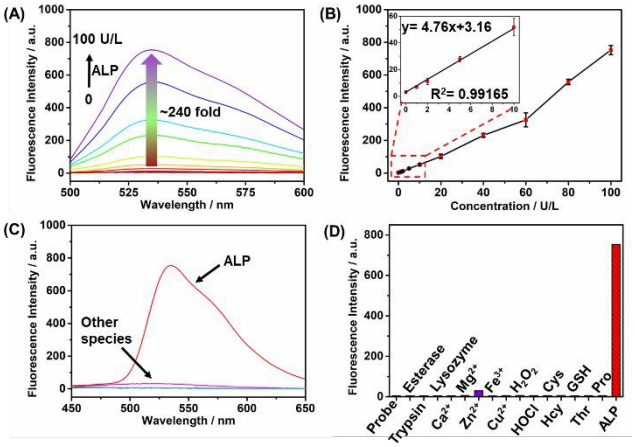

Fig. 3 (A) (Fluorescence spectra of **AE-Phos** (5 μM) in the presence of various concentrations of ALP (0, 1, 2, 5, 10, 20, 40, 60, 80 and 100 U/L) in Tris buffer (pH 9, 50 mM) after 15 min of incubation at 37 °C; (B) Fluorescence intensity changes of **AE-Phos** (5 μM) at 536 nm in the presence of a series of ALP (0-100 U/L). The insert is the linear fitting curve of fluorescence intensity at 536 nm with the concentration of ALP from 0-10 U/L; (C) Fluorescence spectra of **AE-Phos** (5 μM) toward ALP and various interfering substances in Tris buffer (pH 9, 50 mM); (D) Fluorescence responses of AE-Phos (5 μM) at 536 nm toward ALP and various interfering substances in Tris buffer. Esterase (200 U/L), Trypsin (200 U/L), Lysozyme (200 U/L), Ca^{2+}/Mg^{2+}/Zn^{2+}/Fe^{3+}/Cu^{2+} (50 μM), H_2O_2 (100 μM), HOCl (100 μM), Cys (1 mM), Hcy (1 mM), GSH (1 mM), Thr (50 μM), Pro (50 μM), ALP (100 U/L). All species were incubated with AE-Phos at 37 °C for 30 min. Ex: 356 nm.

To examine the feasibility of using **AE-Phos** for quantitative determination of ALP activity, we conducted concentration dependent experiments and monitored dephosphorylation reaction closely. As shown in Fig. 3A, the fluorescence intensity increased with ALP activity in the range of 0-100 U/L after 15 min of incubation. Due to the extremely low background fluorescence of **AE-Phos** in water, the enhanced fluorescence "turn on" ratio was about 240-fold when 100 U/L ALP was used. This is higher than the most reported data in the literatures (Table S1). The experiment also displayed a linear correlation between fluorescence signals at 536 nm and ALP activity from 0 to 10 U/L with the fitting equation y = 4.76x + 3.16 and R^2 = 0.99165 (Fig. 3B). The detection limit is estimated to be 0.012 U/L based on 3σ/slope, which is better than the detection ranges of the most of previously reported fluorescent probes. These results together indicated that **AE-Phos** possess excellent sensitivity for ALP (Table S1).

The specificity of **AE-Phos** towards ALP were also investigated. After reacting with ALP, the fluorescence signals of **AE-Phos** was greatly increased and no obvious change was yet observed with metal ions (Ca^{2+}, Mg^{2+}, Zn^{2+}), reactive oxygen species (H_2O_2, HOCl) and reactive sulfur species (Cys, Hcy, GSH) (Fig. 3C and 3D). The selectivity of **AE-Phos** for ALP versus some commonly observed enzymes was examined as well. These enzymes include esterase, trypsin and lysozyme. Similarly, no obvious fluorescence change was obtained with 30 min of incubation of **AE-Phos** and these enzymes. In addition, the result of inhibitor test also proved that the fluorescence increase was due to the reaction of **AE-Phos** and ALP (Fig. S6). These results demonstrate that **AE-Phos** displays high specificity towards ALP, indicating that the probe holds great potential for specific detection of ALP activity in living cells.

Encouraged by the above result, we further explored

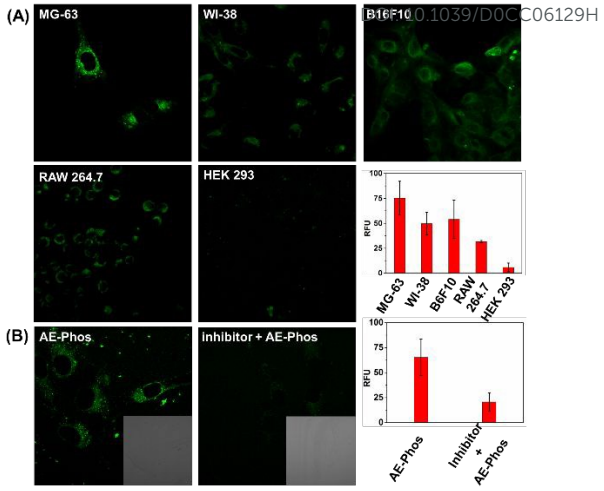

Fig. 4 (A) Confocal fluorescence images of different cells (MG-63, WI-38, B16F10, RAW 264.7, HEK 293) stained with **AE-Phos** (20 μM) after 2 h of incubation; (B) Confocal fluorescence images of living MG-63 cells incubated with **AE-Phos** (20 μM) for 2 h, with or without pre-incubation with 1 mM Na_3VO_4 for 20 min. The columns are the average fluorescence intensities in the cells.

whether **AE-Phos** can differentiate the intracellular ALP activity in different cell lines, such as MG-63, WI-38, B6F10, RAW264.7 and HEK293. Briefly, different cell lines were incubated with **AE-Phos** (20 μM) for 2 h respectively. Fluorescence microscopy was then used to assess the fluorescence intensity. As shown in Fig. 4A, MG-63 cells displayed the strongest fluorescence under the same experimental condition, indicating the highest expression level of ALP in MG-63 among these cell lines. The result is also consistent with the reported literatures, in which the cultured human osteosarcoma cells (MG-63) produce high level of ALP because the transformed osteoblasts in osteosarcoma disrupt the tight control of proliferation and progressively express the cell differentiation genes such as ALP.[11] Cells of WI-38, B16F10 and RAW 264.7 showed moderate fluorescence signal. By contrast, no noticeable fluorescence signal was observed with HEK 293 cells, indicating a lower level of ALP expression, whcih agrees well with the literature.[5a,12] Furthermore, we selected MG-63 cells to investigate the inhibition effect of ALP inhibitor. Specifically, 1 mM Na_3VO_4, an inhibitor of ALP, were incubated in MG-63 cells for 20 min, followed the incubation of **AE-Phos** (20 μM) for another 2 h. The result showed that negligible fluorescence intensity was detected with the cells served with inhibitor, indicating the dephosphorylation of ALP activity was inhibited by Na_3VO_4 (Fig. 4B). Taken together, these results strongly demonstrate that **AE-Phos** is competent to visual imaging endogenous ALP activity in different cell lines.

To examine the fluorescence "turn on" mechanism of **AE-Phos**, the reaction of **AE-Phos** towards ALP was monitored by reversed-phase UPLC (Fig. S7A). Firstly, the retention time of **AE-Phos**, AE-OH-Phos and SA was measured as the standard references. Respectively, the retention time was recorded to be 0.58 min, 1.32 min and 6.36 min. When **AE-Phos** was treated with ALP for 5 min, three peaks belonging to **AE-Phos**, AE-OH-Phos and SA were detected, which indicated AE-OH-Phos was the intermediate product of the reaction. After extending the

incubation time to 20 min, the peak belongs to SA converted to the major product, indicating that dephosphorylation was nearly completed. Furthermore, dynamic light scattering (DLS) analysis revealed that the colloidal aggregates was formed with 249.4 nm average particle diameter for the incubation mixture of **AE-Phos** and ALP (Fig. S7B). However, no colloidal aggregates were observed with **AE-Phos** only in Tris buffer by DLS. Therefore, the reaction mechanism is proposed as follows (Fig. S7C). ALP first catalyses the dephosphorylation of **AE-Phos** to produce intermediate compound AE-OH-Phos, which contains one phosphate group and shows very weak fluorescence. Subsequently, AE-OH-Phos undergoes the second dephosphorylation step and releases **AE-Phos** as the final product, which forms aggregates owing to the intramolecular hydrogen bond and increased hydrophobicity. The aggregation state of SA exhibits strong fluorescent signal due to the combined AIE and ESIPT mechanism.

In summary, a new fluorescent probe, **AE-Phos**, for ALP activity detection in both aqueous buffer and living cells have been constructed herein. After dephosphorylation by ALP, the phosphate groups of **AE-Phos** are removed and the hydroxyl groups are released. The free hydroxyl groups can form intramolecular hydrogen bond with nitrogen atoms, generating stacking of molecules and exhibiting strong fluorescence by AIE and ESIPT effect. The reaction mechanism has been firmly verified by different methods including fluorimeter, UPLC and DLS. Moreover, **AE-Phos** exhibited good water solubility, excellent selectivity and fast response when reacting with ALP. Specially, after reacting with ALP, **AE-Phos** revealed more than 240-fold turn-on ratio and 180 nm Stokes shift, testifying its advantages over most probes in the reported literatures. Most importantly, **AE-Phos** displayed the capability of differentiating and visualizing endogenous ALP activity in different cell lines such as human osteoblastic cells, murine melanoma cells and macrophages.

This work was supported by the National Natural Science Foundation of China (No. 21807014, 21602033), Guangdong Basic and Applied Basic Research Foundation (2020A1515010986, 2020A1515011463), Sichuan Science and Technology Program (2018JY0360), Shenzhen Basic Research Project (JCYJ20180507181654823), the Pearl River Talent Plan of Guangdong Province (2017GC010596).

Conflicts of interest

There are no conflicts to declare.

Notes and references

1 (a) J. E. Coleman, *Annu. Rev. Biophys. Biomol. Struct.,* 1992, **21** 441; (b) J. E. Coleman and P. Gettins, *Adv. Enzymol. Relat. Areas. Mol. Biol.,* 2006, **55**, 381; (c) P. J. Butterworth, *Cell Biochem. Funct.,* 1983, **1**, 66.

2 (a) V. Kermer, M. Ritter, B. Albuquerque, C. Leib, M. Stanke and H. Zimmermann, *Neurosci. Lett.,* 2010, **485**, 208; (b) T. Nakamura, A. Nakamura-Takahashi, M. Kasahara, A. Yamaguchi and T. Azuma, *Biochem. Biophys. Res. Commun*., 2020, **524**, 702; (c) A. Nizet, E. Cavalier, P. Stenvinkel, M. Haarhaus and P. Magnusson, *Clin. Chim. Acta*., 2020, **501**, 198; (d) E. E. Golub and K. B.-Battaglia, *Curr. Opin. Orthop.*, 2007, **18**, 444; (e) K. Poelstra, W. W. Bakker, P. A. Klok, J. A. Kamps, M. J. Hardonk and D. K. Meijer, *Am. J. Pathol.,* 1997, **151**, 1163.

3 (a) W. J. Lammers, H. R. van Buuren, G. M. Hirschfield, H. L. Janssen, P. Invernizzi, A. L. Mason, C. Y. Ponsioen, A. Floreani, C. Corpechot, M. J. Mayo, et.al, *Gastroenterology,* 2014, **147**, 1338; (b) M. Yi, F. Bodola and S. M. Lemon, *Virology,* 2002, **304**, 197; (c) J. J. Stepan, J. Presl, P. Broulik and V. Pacovsky, *J. Clin. Endocrinol. Metab*., 1987, **64**, 1079; (d) S. Poppema, J. D. Elema and M. R. Halie, *Cancer,* 1981, **47**, 1303; (e) Y. Lu, Q. Lu and H. L. Chen, *J. Exp. Clin. Cancer Res.*, 1997, **16**, 75; (f) M. L. Warnock and R. Reisman, *Clin. Chim. Acta*., 1969, **24**, 5.

4 (a) Y. Yang, Q. Zhao, W. Feng and F. Li, *Chem. Rev*., 2013, **113**, 192; (b) J. Chan, S. C. Dodani and C. J. Chang, *Nat. Chem*., 2012, **4**, 973; (c) R. T. Kwok, C. W. Leung, J. W. Lam and B. Z. Tang, *Chem. Soc. Rev*., 2015, **44**, 4228.

5 (a) H. Zhang, P. Xiao, Y.T. Wong, W. Shen, M. Chhabra, R. Peltier, Y. Jiang, Y. He, J. He, Y. Tan, et.al, *Biomaterials,* 2017, **140**, 220; (b) Y. Tan, L. Zhang, K. H. Man, R. Peltier, G. Chen, H. Zhang, L. Zhou, F. Wang, D. Ho, S. Q. Yao, et.al, *ACS Appl. Mater. Inter*., 2017, **9**, 6796; (c) R. Yan, Y. Hu, F. Liu, S. Wei, D. Fang, A. J. Shuhendler, H. Liu, H. Y. Chen and D. Ye, *J. Am. Chem. Soc*., 2019, **141**, 10331; (d) X. Hou, Q. Yu, F. Zeng, J. Ye and S. Wu, *J. Mater. Chem. B,* 2015, **3**, 1042; (e) L. Xu, X. He, Y. Huang, P. Ma, Y. Jiang, X. Liu, S. Tao, Y. Sun, D. Song and X. Wang, *J. Mater. Chem. B,* 2019, **7**, 1284; (f) T. I. Kim, H. Kim, Y. Choi and Y. Kim, *Chem. Commun*., 2011, **47**, 9825; (g) J. Liu, D. Tang, Z. Chen, X. Yan, Z. Zhong, L. Kang and J. Yao, *Biosens. Bioelectron*., 2017, **94**, 271; (h) C. Gao, S. Zang, L. Nie, Y. Tian, R. Zhang, J. Jing and X. Zhang, *Anal. Chim. Acta*., 2019, **1066**, 131; (i) Y. Han, J. Chen, Z. Li, H. Chen and H. Qiu, *Biosens. Bioelectron*., 2020, **148**, 111811; (j) C. Zhang, Q.-Z. Zhang, K. Zhang, L.-Y. Li, M. D. Pluth, L. Yi and Z. Xi, *Chem. Sci.*, 2019, **10**, 1945; (k) Y. Li, H. Song, C. Xue, Z. Fang, L. Xiong and H. Xie, *Chem. Sci.*, 2020, **11**, 5889; (l) S. Gnaim, A. Scomparin, A. Eldar-Boock, C. R. Bauer, R. Satchi-Fainaro and D. Shabat, *Chem. Sci.*, 2019, **10**, 2945.

6 (a) D. Ding, K. Li, B. Liu and B. Z. Tang, *Acc. Chem. Res*., 2013, **46**, 2441; (b) R. Hu, N. L. Leung and B. Z. Tang, *Chem. Soc. Rev*., 2014, **43**, 4494; (c) J. Qian and B. Z. Tang, *Chem*, 2017, **3**, 56; (d) H. Wang, E. Zhao, J. W. Y. Lam and B. Z. Tang, *Mater. Today*, 2015, **18**, 365.

7 (a) A. C. Sedgwick, L. Wu, H. H. Han, S. D. Bull, X. P. He, T. D. James, J. L. Sessler, B. Z. Tang, H. Tian and J. Yoon, *Chem. Soc. Rev*., 2018, **47**, 8842; (b) V. S. Padalkar and S. Seki, *Chem. Soc. Rev*., 2016, **45**, 169.

8 W. X. Tang, Y. Xiang and A. J. Tong, *J. Org. Chem*., 2009, **74**, 2163.

9 (a) L. Peng, M. Gao, X. Cai, R. Zhang, K. Li, G. Feng, A. Tong and B. Liu, *J. Mater. Chem. B,* 2015, **3**, 9168; (b) R. Zhang, M. Gao, S. Bai and B. Liu, *J. Mater. Chem. B,* 2015, **3**, 1590; (c) H. Song, Y. Zhou, H. Qu, C. Xu, X. Wang, X. Liu, Q. Zhang and X. Peng, *Ind. Eng. Chem. Res.,* 2018, **57**, 15216; (d) H. W. Liu, K. Li, X. X. Hu, L. Zhu, Q. Rong, Y. Liu, X. B. Zhang, J. Hasserodt, F. L. Qu and W. Tan, *Angew Chem. Int. Ed*., 2017, **56**, 11788; (e) Y. Li, R. Xie, X. Pang, Z. Zhou, H. Xu, B. Gu, C. Wu, H. Li and Y. Zhang, *Talanta,* 2019, **205**, 120143; (f) M. Gao, Q. Hu, G. Feng, B.Z. Tang and B. Liu, *J. Mater. Chem. B,* 2014, **2**, 3438.

10 D. H. Kohn, M. Sarmadi, J. I. Helman and P. H. Krebsbach, *J. Biomed. Mater. Res*., 2002, **60**, 292.

11 (a) J. Zhou, X. Du, C. Berciu, H. He, J. Shi, Da. Nicastro and B. Xu, Chem, 2016, **1**, 246; (b) J. Delgado-Calle, C. Sañudo, L. Sánchez-Verde, R. J. García-Renedo, J. Arozamena and J. A. Riancho, *Bone*, 2011, **49**, 830.

12 H. Song, Y. Li, Y. Chen, C. Xue and H. Xie, *Chem. Eur. J*., 2019, **25**, 13994.